

available at www.sciencedirect.comwww.elsevier.com/locate/brainres

**BRAIN
RESEARCH**

Research Report
MEG in the macaque monkey and human: Distinguishing cortical fields in space and time
Johanna M. Zumer^{a,b,1}, Srikantan S. Nagarajan^{a,b}, Leah A. Krubitzer^c, Zhao Zhu^{a,c}, Robert S. Turner^{d,2}, Elizabeth A. Disbrow^{a,c,e,*}
^aBiomagnetic Imaging Laboratory, Dept. of Radiology, University of California, San Francisco, CA, USA^bUCSF/UC Berkeley Joint Graduate Group in Bioengineering, San Francisco, CA, USA^cCenter for Neuroscience, University of California, Davis, CA, USA^dDept. of Neurological Surgery, University of California, San Francisco, CA, USA^eDept. of Neurology, University of California, Davis, CA, USA

ARTICLE INFO
Article history:

Accepted 12 May 2010

Available online 20 May 2010

Keywords:

Magnetoencephalography

Monkey

Human

Somatosensory evoked fields

Auditory evoked fields

ABSTRACT

Magnetoencephalography (MEG) is an increasingly popular non-invasive tool used to record, on a millisecond timescale, the magnetic field changes generated by cortical neural activity. MEG has the advantage, over fMRI for example, that it is a direct measure of neural activity. In the current investigation we used MEG to measure cortical responses to tactile and auditory stimuli in the macaque monkey. We had two aims. First, we sought to determine whether MEG, a technique that may have low spatial accuracy, could be used to distinguish the location and organization of sensory cortical fields in macaque monkeys, a species with a relatively small brain compared to that of the human. Second, we wanted to examine the temporal dynamics of cortical responses in the macaque monkey relative to the human. We recorded MEG data from anesthetized monkeys and, for comparison, from awake humans that were presented with simple tactile and auditory stimuli. Neural source reconstruction of MEG data showed that primary somatosensory and auditory cortex could be differentiated and, further, that separate representations of the digit and lip within somatosensory cortex could be identified in macaque monkeys as well as humans. We compared the latencies of activity from monkey and human data for the three stimulation types and proposed a correspondence between the neural responses of the two species. We thus demonstrate the feasibility of using MEG in the macaque monkey and provide a non-human primate model for examining the relationship between external evoked magnetic fields and their underlying neural sources.

© 2010 Elsevier B.V. All rights reserved.

1. Introduction

Studies in humans using non-invasive techniques including functional magnetic resonance imaging (fMRI), magneto-

encephalography (MEG) and electroencephalography (EEG) have provided important information on cortical organization and processing in humans. While some of these non-invasive techniques are indirect measures of neural

* Corresponding author. Center for Neuroscience, 1544 Newton Ct., Davis, CA 95618, USA. Fax: +1 530 757 8827.

E-mail address: liz.disbrow@radiology.ucsf.edu (E.A. Disbrow).¹ Current address: Sir Peter Mansfield Magnetic Resonance Centre, School of Physics and Astronomy, University of Nottingham, UK.² Current address: Department of Neurobiology and Center for the Neural Basis of Cognition, University of Pittsburgh, PA, USA.

function, such as blood oxygenation (e.g. fMRI), more direct measures of neural activity have a lower spatial accuracy (MEG or EEG). However, data on the validity and reliability of these non-invasive techniques are relatively sparse. In examining the capabilities of MEG in the present study we had two aims. First, we sought to determine whether MEG could be used to distinguish the location and organization of sensory cortical fields in macaque monkeys, a species with a relatively small brain compared to that of the human. Second, we wanted to examine the temporal dynamics of cortical responses in the macaque monkey relative to the human.

MEG is a non-invasive tool used to record, on a millisecond timescale, the magnetic field changes generated by neural activity. The basis of the MEG signal is hypothesized to be synchronous cellular currents emanating from parallel apical pyramidal dendrites, based on studies in turtle cerebellar preparations (Lopez et al., 1991; Okada et al., 1987a,b, 1988; Okada and Nicholson, 1988), guinea pig hippocampal preparations (Kyuhou and Okada, 1993; Okada et al., 1997; Wu and Okada, 1998), and in vivo studies in rats (Bau Barth and Di, 1990; Barth and Sutherling, 1988; Barth et al., 1984, 1986). Current flowing through a wire (or dendrite) produces a magnetic field curling around the wire. Thousands to millions of synchronously active neurons with dendrites arranged in parallel produce a magnetic field strong enough to be measured outside the skull. Although MEG signal source location has been estimated using a variety of mathematical models, source localization estimates derived from all models have errors due to the inherently ill-posed inverse problem as well as from other assumptions not met by real data. Based on a realistic phantom study, the resulting spatial uncertainty is estimated to be about 3 mm (Leahy et al., 1998) but may be much larger.

Current data on the feasibility of MEG in the monkey is sparse but promising. In an early study by Teale et al. (1994) auditory evoked fields were recorded using MEG in a pigtail monkey and responses were localized to auditory cortex. More recently, Zhu et al. (2009) and Wilson et al. (2009) examined the response to tactile stimulation of the hand in macaque monkeys measured with MEG and found similar latencies for the initial cortical response (17 ms and 16 ms, respectively).

We used MEG combined with MRI to determine the spatial location of somatosensory and auditory areas of the cortex, as well as the internal somatotopic organization of Brodmann's areas 3b and 1. We measured responses to simple tactile and auditory stimuli using MEG in 4 anesthetized macaque monkeys, and then compared the location of somatosensory and auditory sources with the known location and organization of these fields derived from previous electrophysiological recording studies (Brugge and Merzenich, 1973; Celesia, 1976; Morel et al., 1993; Kaas et al., 1979; Nelson et al., 1980). The use of MEG to determine separate brain regions was demonstrated based on differences in spatial reconstruction localization and latency. For comparison we recorded MEG responses to similar stimuli in human subjects. We estimated the corresponding neural sources using the same source reconstruction methods and compared the latencies of the evoked responses across species.

2. Results

2.1. Monkey MEG evoked responses

Cutaneous stimulation was administered to the digits and lips with a pneumatic diaphragm, and the auditory stimulus was 400 ms of white noise. Evoked response peaks were observed in the averaged MEG sensor time-series data sets for digit, lip and auditory stimulation. A clear response in the sensor data was observed for digit stimulation in 10/10 blocks. Similarly, a clear response from lip stimulation was observed in 12/13 blocks. Auditory stimulation resulted in clear responses in 5/13 blocks. In two monkeys (MK1 and MK3) 4/4 runs showed clear responses. However, only 1/4 auditory blocks showed a clear peak in MK2 and 0/5 auditory blocks in MK4 showed a distinguishable peak. Because the lack of auditory response was restricted to specific monkeys we concluded that the failure to obtain results was not due to technical issues but more likely was related to anatomical factors, such as the location of auditory cortex relative to the sylvian fissure. Similar variability in auditory source localization in humans has been reported previously (Edgar et al., 2003). Examples of tactile and auditory responses from monkey MK1 are shown in Fig. 1 to give an indication of signal-to-noise of sensor data as well as pattern of evoked peaks.

2.2. Monkey MEG latency results

Multiple peaks were observed in the data from each monkey, with some variability in peak magnitude and latency. In the digit data, the most consistent large peak was that seen at 16.4 ms (5.7 ms SD, range 11–27 ms, 9/10 datasets) and this peak was the one selected for source localization of primary somatosensory cortex (Fig. 1, top). An early peak was sometimes measured at 3 ms (7/10); in two of these seven cases this early peak was larger than the 15 ms peak. Later peaks were also seen at 33.0 ms \pm 3.4 ms (range 30–40 ms, 7/10) and at 61.4 ms \pm 11.2 ms (range 47–82 ms, 8/10).

The responses to lip stimulation showed consistent peaks, however the variability in peak amplitude was greater than in the digit response data (Fig. 1, middle). An early peak was observed in 11/12 datasets at 10.5 ms \pm 3.7 ms (range 3–15 ms) and was the largest in 7/12 datasets. This primary peak from lip stimulation had a significantly shorter latency than the primary digit peak ($p < 0.05$). A second peak in the lip stimulation response was seen at 25.4 ms \pm 3.4 ms (range 23–30 ms) in 10/12 datasets and was largest in 3/12 datasets. Finally, a later peak at 49.6 ms \pm 5.0 ms (range 42–57 ms) was consistently observed in 12/12 datasets, and was the largest in 2/12 datasets.

The auditory responses also showed some variability in peak latencies. A peak at 43.5 ms \pm 1.0 ms (range 43–45 ms) was measured in 4/5 datasets and was the largest in 2/5 datasets (Fig. 1, bottom). A slightly later peak was also seen at 60.5 ms \pm 7.1 ms (range 50–65 ms) in 4/5 datasets and was the largest in 3/5 datasets. Finally, a late peak was observed in two cases (77 ms in one case and 110 ms in a second case; combined for a mean of 93.5 ms \pm 23.3 ms).

The overall signal-to-noise ratio was not as high in the monkey data as was observed in human MEG data, but was

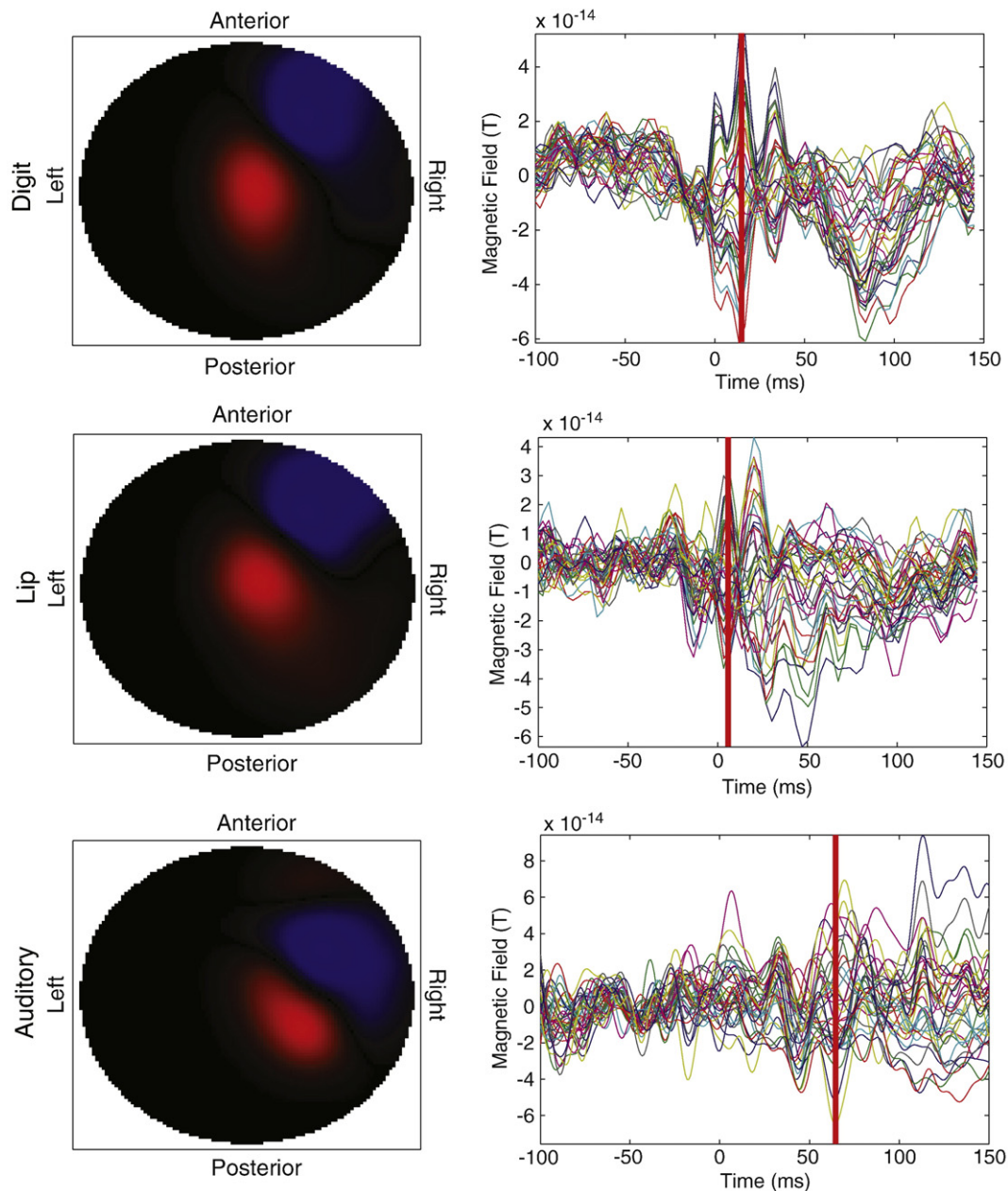


Fig. 1 – Averaged MEG sensor data from monkey MK1. Top row: digit stimulation; middle row: lip stimulation; bottom row: auditory stimulation. Left column: two-dimensional representation of sensor array activity, with conventional representation indicating magnetic field direction (red going into the head and blue out). This field pattern indicates an underlying dipolar source, occurring at the latency of the red vertical bar in the adjacent plot (right). Right column: averaged time-series for magnetic field changes for all 37 sensors, with stimulus onset at time=0 ms. Data shown was filtered from 2–40 Hz.

sufficiently high to detect peaks and perform source localization. Therefore anesthetic may have reduced the monkeys' responses somewhat, but not prohibitively.

2.3. Monkey MEG localization results

The spatial distribution of the beamformer-localized sources in the brain for tactile and auditory stimulation generally agreed with known neuroanatomy (Hackett et al., 2001; Kaas,

1993; see Hackett, 2007 for review). Fig. 2 shows the beamformer source reconstruction for the MEG dataset from MK1. In the data from MK1, the digit localization was 6 mm medial and 8 mm superior to the lip localization on the central sulcus, corresponding to the known location and somatotopic organization of area 3b (Powell and Mountcastle, 1959; Nelson et al., 1980; see Krubitzer and Disbrow, 2008 for review).

The localization of auditory cortex was 12 mm inferior to that of lip stimulation, on the opposite side of the lateral

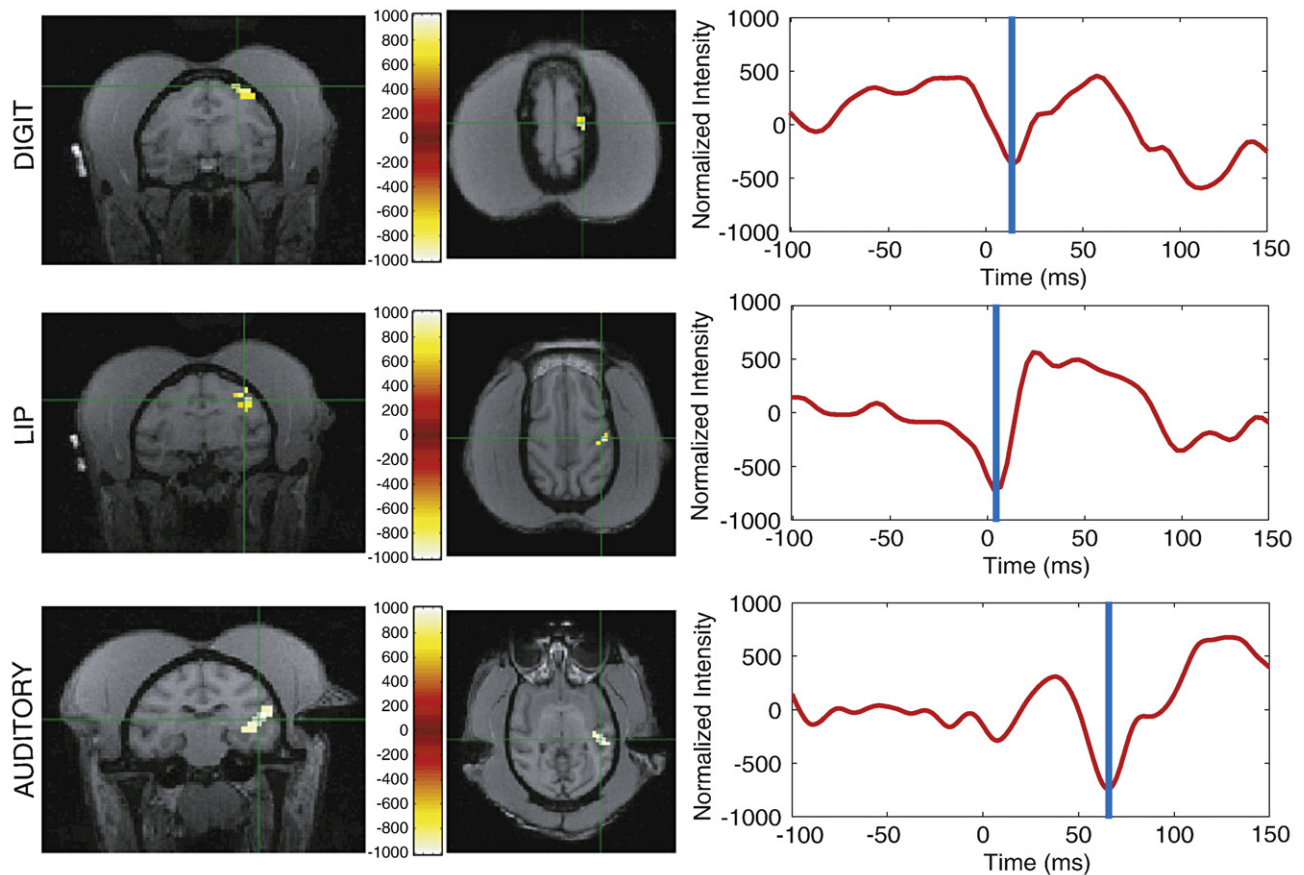


Fig. 2 – Beamformer source localization and time-series of the primary response in the MEG dataset from monkey MK1. Response to digit (top row). Lip (middle row), and auditory (bottom row) stimulation. Left and middle columns: MEG source activity overlaid on coronal and axial MRIs, respectively, occurring at the peak latency indicated by the blue vertical bar in the time-series (right column). The source localization demonstrates that the digits are represented medial to the lip, and that both are represented superior to auditory cortex. Crosshairs on MRIs indicate the voxel with the greatest signal magnitude. Right column: source time-series, estimated by beamforming, at the peak voxel in crosshairs, filtered from 2–40 Hz after beamforming localization. These ‘virtual-electrode’ traces from the most-active voxel for each stimulation type show evoked peaks at the primary latency described in the Results section.

sulcus, likely encompassing the core areas A1 and R. The reconstructed time-series (Fig. 2, right) is shown for the voxel with maximal activation (in green crosshairs on MRI). The largest peak latencies in this example are at 13 ms for digit stimulation, 7 ms for lip stimulation, and 62 ms for auditory stimulation. The peak voxel from this digit localization was about 10 mm anterior to the central sulcus, but the ROI voxels extend posteriorly onto the central sulcus. The lip localization was just on, and slightly posterior to, the central sulcus. The peak voxel was within 2 mm of the central sulcus, which is within the limits of expected error of MEG source localization. The auditory localization was inferior to both digit and lip localization and is wholly contained in the temporal lobe, primarily in the superior temporal sulcus, the known location of primary auditory cortex.

Localization results from the other three monkeys also showed similar spatial arrangement, although the exact spatial locations varied between animals. In 7/10 digit datasets, the beamformer reconstruction produced a spatial

peak in the central sulcus (at least one dataset from each animal). In the remaining three datasets, the source estimates were (1) more medial and inferior (into white matter), (2) more medial and posterior (in white matter and posterior to the central sulcus), or (3) near the central sulcus but relatively low in power. Likewise, 7/12 lip datasets showed activation in the lateral central sulcus (at least one dataset from each animal). The source estimates in the remaining five datasets were (1) posterior to the central sulcus, (2) in the center of the head, (3 and 4) inferior into temporal lobe, or (5) near the central sulcus but relatively weak. Finally, 4/5 auditory data sets were localized to the temporal lobe (in 3/4 monkeys). The remaining localization result was in the most inferior portion of the temporal lobe. The auditory responses were harder to localize as the SNR of the sensor data itself was lower, independent of sensor array type (37 versus 275 channel systems). It is possible that the SNR of AEF responses was lower in monkeys because the source was radial, or because of an increased distance from neural source to the sensors due to the larger

temporal lobe extra-cranial muscle thickness in macaques relative to humans.

The beamformer localization coordinates in the AC–PC coordinate frame (see Experimental procedures) were averaged and compared across stimulation types (10 digit, 12 lip, 5 auditory). Fig. 3 illustrates that the average localization of digit responses was significantly different from lip in the medio-lateral dimension, and digit localization was significantly different from both lip and auditory in the superior–inferior dimension. While lip and auditory localizations were not significantly different from each other, in most cases lip localizations were clearly above the lateral sulcus while auditory localizations were below the lateral sulcus. Note the standard error of the localization ranged between 2–3 mm, well within expected errors of MEG source localization, and indicating overall agreement across animals.

We computed the source orientation for the primary peaks in all monkey datasets (Table 1). While there was consistency within animals, variability was higher across animals. Taking the number of datasets into account and using a randomly-generated distribution of mean unit vector strengths to determine significance, the dipole orientation to lip stimulation did show a significant (above 95th percentile) similarity across datasets, but not for digit or auditory. This mean lip dipole was oriented in a medial, posterior and inferior direction.

2.4. Human MEG evoked responses

Evoked response peaks were observed in the averaged human MEG sensor time-series data sets. Unlike the anesthetized monkeys, a clear response in the sensor data was observed for all digit (4/4), lip (4/4) and auditory (4/4) blocks. The human data showed some variability across subjects similar to the

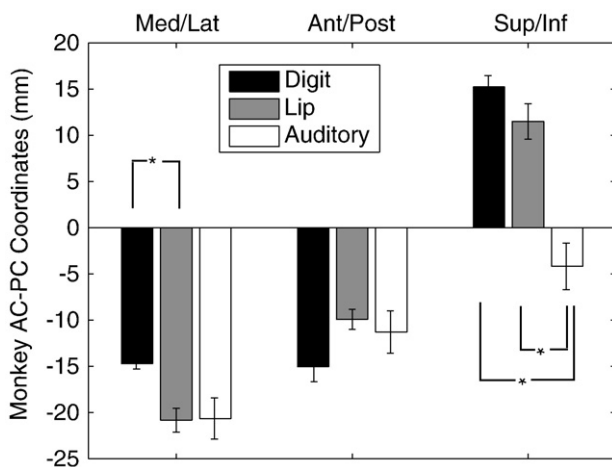


Fig. 3 – Average AC–PC coordinates of all MEG beamformer localization results in monkeys for digit, lip and auditory stimulation. The digit representation is significantly medial to the lip representation and auditory cortex. Further, there was a trend for the digits to be represented slightly posterior to the lip representation and auditory cortex. Finally, both the digits the lips and were significantly superior to auditory cortex. The asterisk indicates pairwise significant difference between means ($p < 0.016$).

variability in the monkey data with respect to peak amplitude and latency.

2.5. Human MEG latency results

In humans it is conventional that well-described peaks in MEG and EEG data are labeled using a number indicating the response latency in milliseconds, prefaced by a letter ‘M’ for MEG data or an ‘N’ or ‘P’ for negative or positive-going amplitudes for EEG data. For digit stimulation, the peak at 44.0 ms \pm 5.0 ms (range 39–50 ms) was largest for all subjects (Fig. 4, top). This peak corresponds to the well-described somatosensory M50 (Hämäläinen et al., 1993; Hashimoto et al., 1999; Kekoni et al., 1992). An early peak was observed in 2/4 subjects at 22.5 ms \pm 0.7 ms (range 22–23 ms) which has also been described elsewhere (Buchner et al., 1994; Disbrow et al., 2001). Later peaks were measured in all subjects clustering at 80 ms \pm 18 ms (range 60–96 ms; 3/4 subjects), at 119.7 ms \pm 3.2 ms (range 116–122 ms; 3/4 subjects), and at 137 ms \pm 4.2 ms (range 134–140 ms; 2/4 subjects). These later peaks around 120 ms probably correspond to the ‘late’ response described in somatosensory data (Disbrow et al., 2001; Hämäläinen et al., 1990; Hari et al., 1983; Kekoni et al., 1992) thought to originate from the second somatosensory area and surrounding cortex.

As in the monkey lip response data, there was more variability in the human lip data regarding peak latency. All (4/4) subjects show an early 19 ms \pm 0 ms peak, which was largest in 2/4 subjects (Fig. 4, middle). All four subjects also showed a peak averaging 37.0 ms \pm 3.7 ms (range 33–42 ms), which was largest for the two remaining subjects. Later peaks were also seen at 55 ms \pm 0 ms (2/4 subjects) and at 106 ms \pm 4.0 ms (range 101–108 ms; 3/4 subjects). The main response to lip stimulation peaked at a shorter latency (37.0 ms \pm 3.7 ms) than the equivalent response to digit stimulation (44.0 ms \pm 5.0 ms), however this latency was not significantly shorter ($p = 0.07$). Previous work suggests that the latency of the response to lip stimulation precedes that of digit stimulation (Baumgartner et al., 1992; Disbrow et al., 2003).

There was also variability in the human auditory data. All subjects showed a peak averaging 105.5 ms \pm 4.5 ms (range 102–112 ms), consistent with the auditory M100 commonly reported (Pantev et al., 1990) as well as a peak averaging 162.0 ms \pm 10.1 ms (range 153–175 ms; Fig. 4 bottom). The M100 peak was largest in 2/4 subjects; the other two subjects showed the largest peak at \sim 162 ms. Two subjects showed an early peak averaging 58 ms \pm 4.2 ms (range 55–61 ms), consistent with the auditory M50 reported elsewhere (Reite et al., 1988). All four subjects also showed a later peak at 200.8 ms \pm 5.4 ms (range 195–208 ms), consistent with the auditory M200 (Jacobson et al., 1991).

2.6. Human MEG localization results

The localization results from the human MEG data were in agreement with previous MEG studies of somatosensory and auditory stimulation in humans (Hämäläinen et al., 1993; Hari et al., 1984) and with the monkey data described above. The averaged sensor data for digit, lip and auditory stimulation

Table 1 – Mean orientations of dipole sources for each stimulation type and species. The mean of the dipole orientations are reported both for each of the 3 cardinal directions as well as radial magnitude. As defined by AC–PC coordinates for the monkeys and MNI coordinates for humans, mean directions are reported for the Left/Right (right=positive), Anterior/Posterior (anterior=positive), and Superior/Inferior (superior=positive). Random sets of vectors were averaged to create a probability density function to determine the 95th and 99th percentile (furthest right columns), as a function of number of datasets (vectors) averaged together. The mean magnitude is in bold if above the 95th percentile threshold.

	L/R	A/P	S/I	Magnitude	#Datasets	95%	99%
Monkey							
Digit							
Mean	0.36	−0.34	0.11	0.50	10	0.51	0.66
SD	0.52	0.61	0.43				
Lip							
Mean	0.34	−0.22	−0.23	0.47	12	0.47	0.60
SD	0.52	0.45	0.62				
Auditory							
Mean	0.41	−0.09	0.28	0.50	5	0.72	0.88
SD	0.39	0.58	0.67				
Human							
Digit							
Mean	−0.58	−0.69	−0.41	0.99	4	0.80	0.93
SD	0.07	0.10	0.08				
Lip							
Mean	−0.59	−0.55	−0.35	0.88	4	0.80	0.93
SD	0.41	0.30	0.22				
Auditory							
Mean	−0.22	−0.47	−0.22	0.56	4	0.80	0.93
SD	0.54	0.37	0.69				

from one human subject (HU4) are shown in Fig. 4, while Fig. 5 shows the estimated beamformer source localization and the corresponding estimated temporal activity from the same datasets. Both digit and lip localizations are entirely on the post-central gyrus with the lip representation lateral and inferior to digit; the auditory localization in Fig. 5 is in the superior temporal sulcus.

The average MNI coordinates from all four subjects are shown in Fig. 6. The digit localization was more superior and posterior than the lip localization, although only significantly different in the anterior–posterior dimension. The auditory coordinate was found to be significantly inferior to both digit and lip representations.

We also computed the source orientation for the primary peaks in all human datasets (Table 1). The orientation of the digit dipoles was highly consistent across subjects (magnitude of mean of unit vector orientations above 99th percentile) and also significant for lip stimulation (above 95th percentile), but not for auditory dipoles. Both the digit and lip dipoles were similarly oriented, pointing in a lateral, posterior and inferior direction. Both digit and lip dipoles within each species were similar. However, it has been shown that auditory dipoles in humans can be quite variable (Edgar et al., 2003), which is consistent with the variability seen here in the auditory dipoles in both species.

3. Discussion

We have demonstrated that MEG is a robust, non-invasive tool for distinguishing the spatial location and internal organiza-

tion of cortical fields in macaque monkeys as well as humans. This finding is important because MEG is best known for studies of neural temporal processing. In addition, the latencies of tactile and auditory responses recorded using MEG in monkeys showed a pattern similar to human data, though latencies were shorter in monkeys. Finally, the pattern of variability in latency and morphology of responses was similar across species. In the following discussion we compare the latency and localization data from digit, lip and auditory stimulation from our MEG study to existing data from monkeys and humans.

3.1. Monkey and human responses: comparisons of response latencies

MEG, EEG and electrocorticography (ECoG) are sensitive to the same underlying neural process (Hämäläinen et al., 1993), and while EEG and MEG display differing spatial sensitivities (Cuffin and Cohen, 1979), a given response will occur at the same latency using both methods (Fuchs et al., 1998; Nagamine et al., 1998; Sharon et al., 2007). Thus, we compare our findings with the latencies reported from a wealth of subdural or scalp EEG recordings as well as less widely available MEG latency data (Table 2).

Our data on response latency of digit stimulation are in agreement with existing evoked potential data from macaque monkeys. McCarthy et al. (1991) recorded subdurally from macaque monkeys during median-nerve stimulation and found an N10–P20 wave generated from area 3b and a P12–N25 wave from area 1 in monkeys. Similarly, Kulics and Cauller (1986) presented electrical cutaneous stimulation to

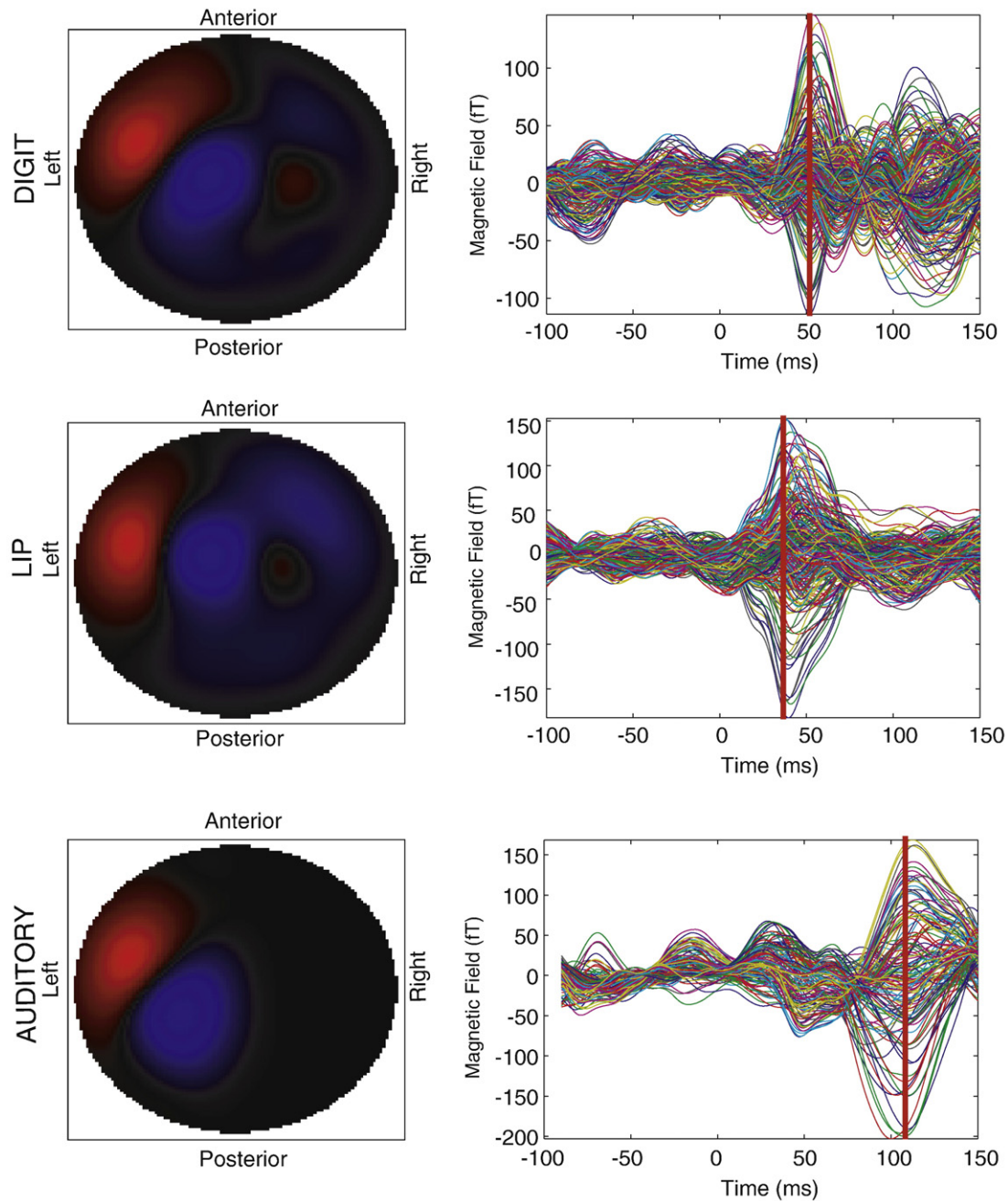


Fig. 4 – Averaged MEG sensor data from human subject HU4. Top row: hand stimulation; middle row: lip stimulation; bottom row: auditory stimulation. Left column: two-dimensional representation of sensor array activity, with conventional representation indicating magnetic field direction (red going into the head and blue out). This field pattern indicates an underlying dipolar source pattern, occurring at the latency of the red vertical bar in the adjacent plot (right). Right column: averaged time-series of magnetic field changes for all sensors, filtered from 2–40 Hz, with stimulus onset occurring at time=0 ms. Digit and lip plots show overlay of all 275 sensors used in beamformer analysis; auditory plot shows only the left 132 sensors used in beamformer analysis.

macaque monkeys and report two negative deflecting peaks at 12 ms and 20 ms and a positive peak around 50 ms, which they show come from different cellular layers within area 3b from cortical source density (CSD) measurements. Previous studies in humans (Allison et al., 1989; Wood et al., 1988) have

examined the cortical origin of evoked median-nerve stimulation responses using subdurally-placed electrodes in patients requiring neurosurgery. They found the strongest and earliest peak in area 3b (N20–P30), with area 1 peaking 5 ms later (P25–N35). Thus, McCarthy, Allison and colleagues

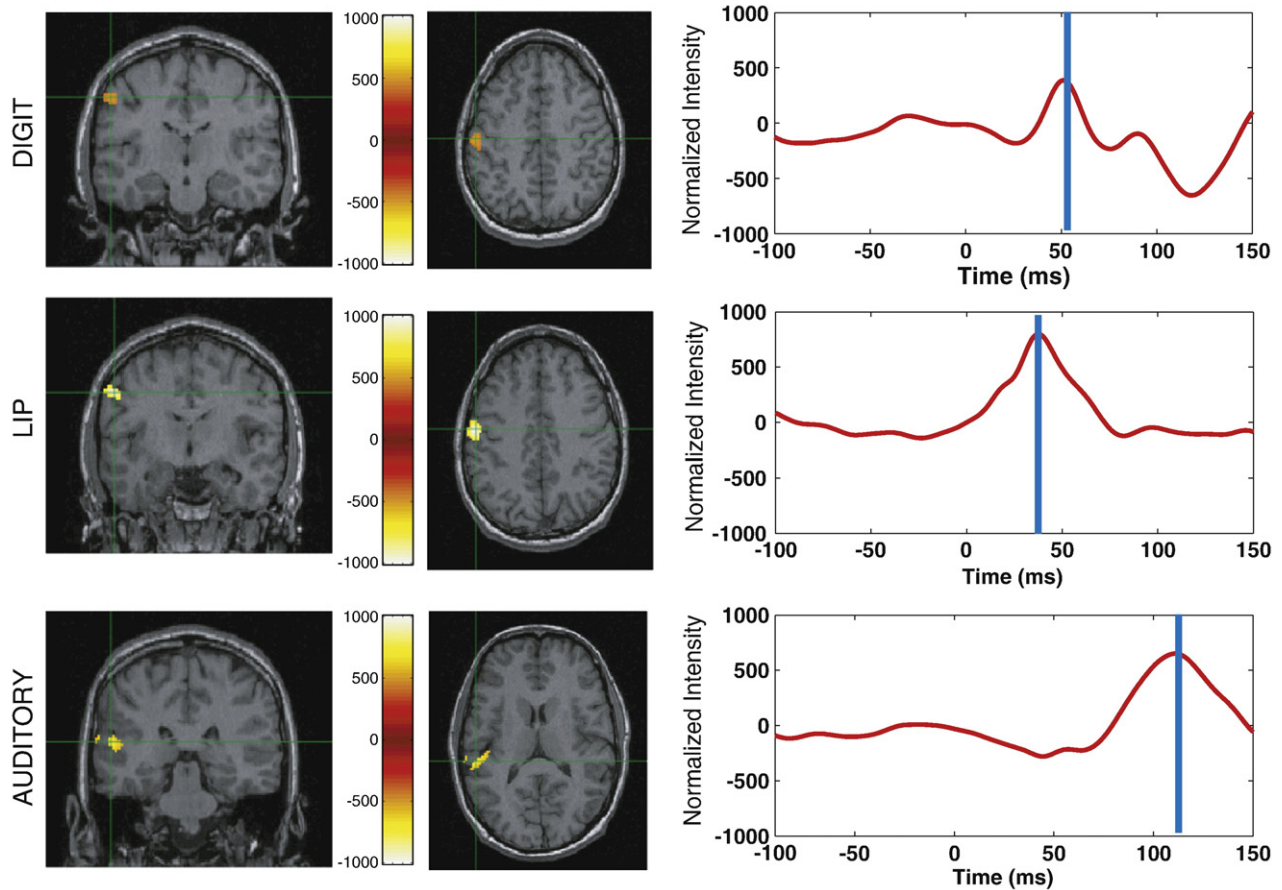


Fig. 5 – Beamformer source localization and time-series for primary responses in human HU4 MEG dataset. Top row: digit localization; middle row: lip localization; bottom row: auditory localization. Left and middle column: MEG source activity overlaid on coronal and axial structural MRIs, respectively, occurring at the peak latency indicated by the blue vertical bar in the adjacent time-series (right column). Crosshairs on the MRI indicate the voxel with the largest magnitude activity. The source localization demonstrates that the digits are represented superior to the lip, and that both are represented superior to auditory cortex. Right column: source time-series estimated by beamforming at the peak voxel in crosshairs, filtered from 2–40 Hz after beamforming localization. These ‘virtual-electrode’ traces from the most-active voxel for each stimulation type show evoked peaks at the primary latency described in the results.

(McCarthy et al., 1991; Allison et al., 1991) proposed the monkey N10–P20 and P12–N25 to be the correlates of the human N20–P30 and P25–N35.

We propose that the 15 ms peak seen in our monkey MEG digit data corresponds to the 40 ms wave in human MEG data of digit stimulation observed in our data and elsewhere (Disbrow et al., 2001; Hämäläinen et al., 1993; Hashimoto et al., 1999; Kekoni et al., 1992). It is also likely that the sometimes-seen earlier peak at 3–10 ms in the monkey MEG data corresponds to the sometimes-seen 20 ms peak in the human MEG data for tactile digit stimuli, and that the later 30 ms/40 ms peak in the monkey responses corresponds to the human 80 ms peak which likely emanates from S2 and surrounding cortex (Table 2; Disbrow et al., 2001; Hämäläinen et al., 1990; Hari et al., 1984).

In monkeys, previous work recording intracranial somatosensory evoked potentials (SEP’s) using electrical stimulation applied to median nerve, lip, tongue and palate showed that, as in our study, latencies were slightly shorter for lip relative to

hand responses (N9–P14 for lip and N10–P20 for hand; McCarthy and Allison, 1995). In humans, the evoked fields resulting from lip stimulation show a clear ~20 ms peak as well as a later ~35 ms peak (Table 2; Disbrow et al., 2003; Hoshiyama et al., 1996; Nakahara et al., 2004; Nakamura et al., 1998) with latencies for the lip response shorter than the digit response (Baumgartner et al., 1992). It is likely that the monkey ~10 ms and ~25 ms peaks observed here from lip stimulation correspond with the human ~20 ms and ~35 ms peaks respectively.

More variability was seen in later peaks than early peaks for hand, lip and auditory stimulation across studies. For example, Gardner et al. (1984) presented air-puff stimuli to the hand or forearm of alert macaque monkeys while recording epidural SEPs. They found P15 and P25 peaks followed by a large N43 and P70. Their early peak matches the early peak (16 ms) in our data; however, the later peaks do not match well (33 ms and 61 ms). Later peaks tend to be more variable across individual subjects, as in the present study, and are likely affected by anesthesia. In addition, median-nerve stimulation

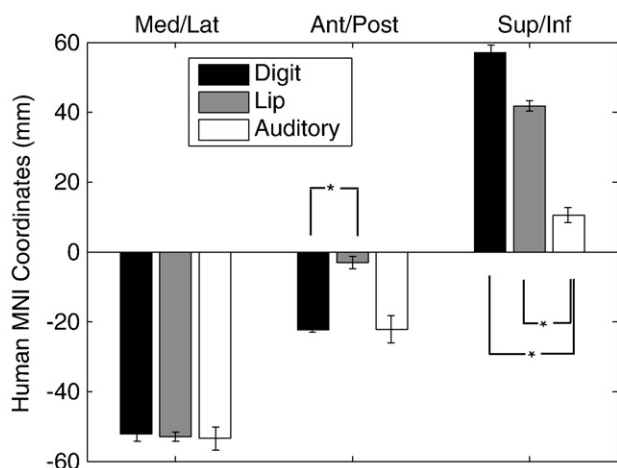


Fig. 6 – Average MNI coordinates of MEG beamformer localization results in humans for digit, lip and auditory stimulation. These coordinates indicate that the lip representation is significantly anterior to the digit representation in S1. Both digit and lip representations were significantly superior to auditory source location. The asterisk indicates pairwise significant difference between means ($p < 0.016$).

evokes a response about 5–10 ms earlier than cutaneous stimulation to the hand (e.g. compare Gardner et al. (1984) to Arezzo et al. (1981) recording intracranially in the monkey or human MEG data from Forss et al. (1994)).

In the auditory system, Arezzo et al. (1975) measured early (12–22 ms) auditory evoked potentials (AEPs) in response to auditory clicks in the monkey using chronically implanted electrodes on the supratemporal plane. These responses originated from primary auditory cortex (A1). Later AEPs (N40 and N60) arose from areas on the superior temporal plane more anterior to A1, and the N70 and N100 arose from more posterior areas. Similarly, Teale et al. (1994) measured responses to an auditory tone at 22 ms, 46 ms, and a slightly later 130 ms using MEG in the monkey. Both of these studies are consistent with the auditory responses we recorded using MEG in monkeys at 44 ms, 61 ms, and 94 ms (Table 2). We propose that the early 44 ms peak in the monkeys corresponds to the earlier auditory M50 in humans.

Evidence exists that the human auditory N100 (and corresponding M100) in particular seems to arise from either A1 or the planum temporale (Godey et al., 2001; Liegeois-Chauvel et al., 1994). Furthermore, Arezzo et al. (1975) proposed that the monkey N70 corresponds to the human N100, which they suggest has a dual origin in A1 and posterior regions in both species. Our data, which showed large peaks in monkeys at 61 ms, are consistent with this hypothesis, particularly because secondary auditory areas adjacent to and surrounding the core (A1 and R), such as the belt and parabelt areas, are likely activated by the noise stimuli presented in this study (Rauschecker et al., 1995; Rauschecker and Tian, 2004; Patterson et al., 2002 and Wessinger et al., 2001).

The later auditory peaks were more variable; however, it is possible that the 94 ms peak reported here in monkeys

corresponds to the 100 ms peak found by Arezzo et al. (1975) in monkeys, which furthermore may correspond to the human auditory peak at 150 or even 200 ms. Human data (Chait et al., 2004) supports the idea that the 94 ms peak that we measured in response to noise stimulation in the monkey corresponds to the human M150, which was of relatively large amplitude in response to noise vs. tone stimulation.

Latency differences between species for homologous neural responses can be influenced by conduction distances as well as axon diameter. Within cortex, the roughly doubling of latencies between macaques and humans can mostly be attributed to a difference in conduction speeds, with evidence from an elegant study by Caminiti et al. (2009). Caminiti et al. (2009) showed that cortical conduction speeds were roughly double for humans compared to macaques for both motor-to-midline and prefrontal-to-midline measurements, and that this doubling corresponded to increased axon diameter found in human cortex. However, the doubling of arm length between species (70 cm for humans (Eyre et al., 1991) and 33 cm for macaques (Hamada et al., 2005)) likely contributes to differences in response latency for digit stimulation as well.

Taken together, the data from the present investigation as well as previous studies in humans and monkeys indicate that response latencies can be reliably compared across studies, species and areas, and that the relative spatial and temporal pattern of activity in primary somatosensory and auditory cortex is similar in both humans and macaque monkeys.

3.2. Neuroanatomic variation in cortical field location

In somatosensory cortex we were able to distinguish the digit representation as superior to the lip representation along the central sulcus. These results are in agreement with the known organization of somatosensory cortex with a representation of the body along the post-central gyrus (Nelson et al., 1980; Penfield and Boldrey, 1937; Wood et al., 1988; see Krubitzer and Disbrow, 2008 for review), with the foot representation most medial and superior, and the hand and then face representation at the most lateral and inferior portion. Our source location findings for auditory cortex are also in agreement with the location of auditory cortex described in previous work (Brugge and Merzenich, 1973; Celesia, 1976; Morel et al., 1993).

However, while we could distinguish primary sensory areas based on location, there was some variability in the mean locations across stimulation runs and individuals. The standard error of the mean of the A–P, S–I, and L–R directions for each of digit, lip and auditory stimulation ranged from 1–3 mm in monkeys and 1–5 mm in humans (Figs. 3 and 6). While these errors are within the normal variability seen in MEG source localization, they can be large with respect to sulcal and gyral landmarks. Some of the variability may have been technical; however, some is likely due to natural neuroanatomic variation across subjects.

Our tactile stimulus activated neurons in areas 3b and 1, and possibly area 2 as well. Since neurons in area 3b are generally located in the posterior bank of the central sulcus, their tangential orientation relative to the surface of the head make them a likely source of the MEG signal, while the radially-oriented source from neurons in area 1 on the crown of the post-central gyrus are least likely to be detected with

Table 2 – Summary of the studies measuring responses latencies to hand, lip or auditory stimulation using MEG or intracranial electrodes from monkeys and humans. Columns are arranged to relate peaks across studies and across species. For the present study (in bold font), mean (standard deviation) are reported. All other studies are reported as either the mean or a standard peak (e.g. ‘M100’). For the hand, when somatosensory stimulation type was electrical, the median nerve was stimulated unless otherwise indicated.

Table	Stimulus	Recording	Digit peaks (ms)				
<i>Monkey</i>							
Present	Cutaneous	MEG	3.0 (0.0)	16.4 (5.7)	33 (3.3)	61.4 (11.2)	
Zhu et al. (2009)	Cutaneous	MEG	10	20	37		
Wilson et al. (2009)	Cutaneous	MEG		16		96	
Gardner et al. (1984)	Cutaneous	Intracranial		15	25	43	70
Arezzo et al. (1981)	Electric	Intracranial		10	24	45	110
Kulics et al. (1986)	Electric (finger)	Intracranial		12	20	50	
McCarthy et al. (1991)	Electric	Intracranial		10			
McCarthy et al. (1995)	Electric	Intracranial		10	20		
<i>Human</i>							
Present	Cutaneous	MEG	22.5 (0.7)	44.0 (5.0)	80.3 (18.4)	119.7 (3.2)	137 (4.2)
Hari et al. (1985)	Cutaneous	MEG		45	60		
Forss et al. (1994)	Cutaneous	MEG	32	44	64	106	
Nakamura et al. (1998)	Cutaneous	MEG		46		120	
Hashimoto et al. (1999)	Cutaneous	MEG	23	47	90		
Disbrow et al. (2001)	Cutaneous	MEG	20	40	80	100	
Kekoni et al. (1992)	Electric (finger)	MEG/EEG		56		114	
Hari et al. (1984)	Electric	MEG		30	45	75	
Forss et al. (1994)	Electric	MEG	20	35	57	101	
Buchner et al. (1994)	Electric	MEG/EEG	20	30	45		
Nakahara et al. (2004)	Electric	MEG	23				
Allison et al. (1989)	Electric	Intracranial	20		45	80	180
Baumgartner et al. (1992)	Electric	Intracranial	20	35			
	Stimulus	Recording	Lip peaks (ms)				
<i>Monkey</i>							
Present	Cutaneous	MEG	10.5 (3.7)	25.4 (3.4)	49.6 (5.0)		
McCarthy et al. (1995)	Electric	Intracranial	11	18			
<i>Human</i>							
Present	Cutaneous	MEG	19.0 (0.0)	37.0 (3.7)	55.0 (0.0)	106 (4.0)	
Nakamura et al. (1998)	Cutaneous	MEG		34	60		
Disbrow et al. (2003)	Cutaneous	MEG	10	30	55	110	
Hoshiyama et al. (1996)	Electric	MEG	20	40	60	80	110
Nakahara et al. (2004)	Electric	MEG	15		53		
Baumgartner et al. (1992)	Electric	Intracranial	15	25	40		
	Stimulus	Recording	Auditory peaks (ms)				
<i>Monkey</i>							
Present	Noise	MEG		43.5 (1.0)	60.5 (7.1)	93.5 (23.3)	
Teale et al. (1994)	Tone	MEG	22	46			130
Arezzo et al. (1975)	Click	Intracranial	22	38	60/73	100	140
<i>Human</i>							
Present	Noise	MEG		58.0 (4.2)	106.0 (4.5)	162.0 (10.1)	201.0 (5.4)
Hari et al. (1987)	Noise	MEG		40	100	200	200
Pantev et al. (1990)	Tone	MEG			100		200
Reite et al. (1988)	Tone	MEG/EEG		48	100	150	
Jacobson et al. (1991)	Tone	MEG			105		182
Godey et al. (2001)	Tone	MEG	33	52	92	158	
Godey et al. (2001)	Tone	Intracranial	34	51	91	152	244
Liegeois-Chauvel et al. (1994)	Tone	Intracranial	30	50/60/75	100		

MEG (Hämäläinen et al., 1993). However, the location of cortical fields can be shifted dramatically relative to the sulcus (Krubitzer et al., 2004; Roland and Zilles, 1998; Caspers et al., 2006). For example, 3a has been observed in different

monkeys on the anterior bank, in the depth, or on the posterior bank of the sulcus (Krubitzer et al., 2004). Thus it is likely that normal variability in cortical field location and sulcal anatomy play a role in the observed variability.

Our MEG latency and localization results are consistent with the assertion that the posterior bank of the central sulcus is the cortical origin of the large early peak seen in MEG data. However, previous work mentioned above suggests an early response in area 3b followed shortly by a response in area 1, in both monkeys and humans (McCarthy et al., 1991; Allison et al., 1989; Wood et al., 1988). The combination of factors, the response from area 1 closely following that from area 3b, and the possible shifting of fields with respect to the sulcus could lead to variability in source localization and latency across subjects.

3.3. Adding MEG to the brain mapping toolbox: advantages and challenges

In humans, MEG is increasingly used for spatiotemporal mapping of brain function. However, validation efforts lag behind the widespread use of this technique. A few studies have compared human MEG data to electrocorticography (ECoG) obtained in patients requiring neurosurgery and have shown good correspondence in spatial, temporal and frequency domains between the measures, especially for task-based paradigms in the lower frequency bands, which have inherently higher SNR (Dalal et al., 2008; Halgren, 2004; Sutherling et al., 1988). However, these studies, as a tool for MEG validation, are limited by ECoG electrode placement and the rare use of depth electrodes. Further, brain disease is a potential confounding factor in these studies. Thus, the challenge remains to provide validation of MEG results.

In the present investigation, we used MEG combined with MRI to determine the spatial location of somatosensory and auditory areas of the cortex, as well as the internal somatotopic organization of 3b/1. In addition, MEG also offers high temporal resolution so that the temporal profile of activity in a given cortical field or across fields can be measured. In fact, this temporal profile can be used to infer the site of integration of inputs as well as cortical connectivity. It is critical to examine the organization and function of the neocortex using multiple criteria (Kaas, 1983), and MEG is a powerful tool in overcoming the hurdles of studying the human brain non-invasively, yielding information about multiple characteristics of a cortical field that have been difficult to obtain in the same subject using non-invasive techniques. MEG data provide the location and amplitude of activity in a given cortical field, exquisite temporal information about neural response properties in that field, as well as insight into cortical connectivity, all of which can now be validated in the monkey model.

4. Experimental procedures

Four adult male macaque monkeys (9–15 kg) were scanned using MEG and MRI on separate days. Four healthy human volunteers (3 male and 1 female, ages 23–28) also participated in both MEG and MRI experiments which were performed on separate days. All studies were performed with approval of the UCSF Institutional Animal Care and Use Committee or the Committee on Human Research.

4.1. Stimuli

Calibrated tactile stimulation was delivered using compressed air-driven balloon diaphragms clipped onto either the digits or lips. Stimulus intensity was 25 psi for monkeys and 18 psi for humans, and stimulus duration was 140 ms with a rise time of 30 ms for both hand and lip in both species. For hand stimulation in the monkey, two clips delivering simultaneous stimulation were placed on the tip of the thumb (digit one, D1) and the thenar area. Three monkeys (MK2, MK3 and MK4) were stimulated on the right hand and the other monkey (MK1) on the left hand. In the human, four clips delivering simultaneous stimulation were placed on the subject's right hand: one each on the distal and middle segments of D2 and D3.

For lip stimulation in the monkey, two clips were placed on the lateral upper and lower lips, on the same side as the hand that was stimulated. In the human, two clips were placed on the right lateral upper lip and two clips on the right lateral lower lip. All four lip sites were stimulated simultaneously.

All tactile stimuli were presented in blocks of 256 trials with an inter-trial interval (ITI) of 1000 ms \pm 50 ms for monkeys and 500 ms \pm 50 ms for humans. Low level white noise was presented continuously to the human subjects during tactile stimulation via binaural earplugs to mask and thereby reduce the effect of sounds made by the balloon diaphragms; monkeys wore earplugs for this purpose.

Auditory stimulation for both species consisted of bursts of white noise (350 Hz to 17.6 kHz, 400 ms duration, 5 ms rise time) delivered via binaural earplugs, with 128 epochs per block and an ITI of 1500 ms \pm 50 ms.

4.2. MEG acquisition — monkeys

Macaque monkeys were initially anesthetized using intramuscular (I.M.) injections of ketamine hydrochloride (10 mg/kg), and anesthesia was maintained with intravenous (I.V.) or I.M. boluses of ketamine hydrochloride administered every 15–30 min (3–5 mg/kg/h) and optionally boluses of I.V. midazolam (0.05–0.36 mg/kg/h). Heart rate, respiratory rate, temperature and SpO₂ were documented every 30 min. Heated water bottles and blankets were used to keep the animal warm. An experimenter stayed in the shielded room to monitor the monkey at all times. Any large movements, such as a cough or yawn, were noted and that data block was not analyzed. Sessions lasted 4–6 h including preparation time, and animals recovered in their home cage.

Two separate MEG scanners were used to collect data from the macaque monkeys. Both scanners were located in a shielded room. For two monkeys (MK1 and MK2) a 37-channel magnetometer (BTi, San Diego, CA) was used. Each monkey's head geometry, specifically the bony portions of the forehead and longitudinal fissure, was recorded using a digital sensor position indicator (FASTRAK, by Polhemus, Colchester, VT). Central forehead and left and right preauricular points were identified as landmarks to define the MEG spatial reference frame for later coregistration with the structural MR image. The sensor array was centered over the central sulcus contralateral to the site of stimulation.

Somatosensory data were collected in 300 ms epochs, with 150 ms pre-stimulus period, sampled at 300 Hz. Auditory data were collected in 600 ms epochs, with 100 ms pre-stimulus, sampled at 1 kHz. Multiple data sets were obtained from each monkey. MK1 was scanned on two separate days while MK2 was scanned on one day.

To scan monkeys' MK3 and MK4, a 275-channel CTF Omega 2000 system with 3rd-order gradient correction (VSM MedTech, Coquitlam, B.C., Canada) was used. Three localizing coils were attached to the central forehead and 1 cm anterior to the left and right preauricular points. At the start and end of each trial, current ran through the coils to permit precise localization of these three fiducial points relative to the sensor array. These fiducials were later coregistered with the high-resolution structural MR image.

Somatosensory data were collected in 400 ms epochs, with a 150 ms pre-stimulus period, sampled at 1200 Hz. Auditory data were collected in 600 ms epochs with 100 ms pre-stimulus period, and were sampled at 1200 Hz. MK3 was scanned on two separate days and MK4 was scanned on three separate days.

4.3. MEG acquisition — humans

All human subjects were scanned using the same 275-channel CTF Omega 2000 system used for monkeys MK3 and MK4. The localizing coils were attached to the subject's head prior to placement in the whole-head helmet sensor array. One coil was placed at the nasion, and two additional coils were placed 1 cm anterior to the left and right preauricular points. As in the monkey scans, the position of these coils was measured relative to the sensor array before and after every block of trials. In all blocks, the subjects moved less than the criterion of 5 mm. These points were later coregistered with the high-resolution structural MR image.

Somatosensory data were collected in 400 ms epochs, with a 150 ms pre-stimulus period, sampled at 1200 Hz. Auditory data were collected in 600 ms epochs with 100 ms pre-stimulus period, and were sampled at 1200 Hz. One data set was obtained from each human subject collected in a single session.

4.4. MRI acquisition — monkeys

Macaque monkeys were initially anesthetized using I.M. ketamine hydrochloride (10 mg/kg). Once anesthetized, the animals were cannulated and intubated. Throughout the experiment the animals received lactated Ringer's solution (10 mL/kg/h) and anesthesia was maintained using 1–2% Isoflurane. Atropine sulfate (0.04 mg/kg) was also given I.M. to help reduce secretions. Temperature was maintained and vitals were monitored as described above for the MEG experiments.

All MR scans were performed on a GE Signa 1.5 T scanner (GE, Milwaukee, WI). The monkeys were placed in the prone position and their heads were secured in an MR-compatible stereotaxic frame. A 5 in. diameter surface coil was placed on the superior part of the head. Donut-shaped MR-contrast fiducials were placed in the same three positions as the localizing coils in the MEG session to assist in coregistration. After a sagittal localizing scan, a 3D-SPGR image was acquired with a flip angle of 40°, TR of 27 ms, TE of 7 ms, FOV of

190×190mm with 256×256×124 pixels with an in-plane resolution 0.74 mm×0.74 mm and a slice thickness of 1.0 mm.

4.5. MRI acquisition — humans

All MR scans were performed on the same GE Signa 1.5 T scanner that was used for the monkey scans. A standard GE birdcage volume coil was used and as in the monkey scans. Donut-shaped MR-contrast fiducials were placed on the subjects' head in the same positions as the localizing coils in the MEG session to assist in coregistration of MEG and MR datasets. After a sagittal localizing scan, a 3D-SPGR image was acquired using a flip angle of 40°, a TR of 27 ms, a TE of 6 ms, a FOV=240×240mm, 256×256×124 pixels with an in-plane resolution 0.94 mm×0.94 mm and a slice thickness of 1.5 mm.

4.6. MEG processing — monkeys

To produce comparable data sets we used only the 37 channels closest to the cortical region of interest for MK3 and MK4 scanned in the 275-channel MEG system. The sensor spacing of the 275-channel system is identical to that of the 37-channel system, so both MEG machines provided comparable information. Further, because the monkey's head was relatively small, most of the sensors in the 275-channel system were not near the head and were therefore recording predominantly noise, and only the hemisphere near the sensors contributed to signal in the recordings.

To localize neural sources we chose to use a beamformer technique, specifically the eigenspace beamformer. The eigenspace beamformer has been shown to be more robust than dipole fits (Gutierrez et al., 2006; Sekihara et al., 2002). While an equivalent current dipole (ECD) inverse method has been used extensively, and we have used it successfully with high SNR SEF monkey data (Zhu et al., 2009), it has been shown to be equivalent to beamforming for high SNR data (Gaetz and Cheyne, 2003). However, for lower SNR data, the eigenspace beamformer is more robust to errors in the forward lead field (Sekihara et al., 2002). Therefore, we chose to use the eigenspace beamformer for this data which could be relatively noisy.

Data processing was carried out using NUTMEG (Dalal et al., 2004; <http://nutmeg.berkeley.edu>). The raw sensor data was averaged and the mean of the pre-stimulus period was subtracted from the whole waveform. Only the runs with clear responses in the sensor data were processed for source localization and further quantification of latency and localization.

The fiducial points or digitized headshape were coregistered with the structural MRI. A volume-of-interest (VOI) was defined to include the whole cerebrum and a grid size of 2 mm was used. The source power was estimated over the whole cerebrum so that the maximum activation relative to other regions could be determined. The forward lead field was calculated for the whole cerebrum using a single-shell spherical volume conductor model.

To determine the optimal location of the sphere center, we examined additional data sets and compared a head based location to a sensor based location. The result was a sphere center location near the center of the monkey's head that was

slightly skewed in the direction of the center of the sensor curvature. This location was optimal for both SEF and AEF data.

An adaptive spatial filtering algorithm, specifically the eigenspace vector beamformer, was used for MEG source localization (Sekihara et al., 2001). The time course and power of neural activity at each grid point (voxel) was estimated using a weight matrix (a data dependent spatial filter), applied to the sensor data. To determine the weight matrix the time window containing roughly the first 50–70 time points post-stimulation of unfiltered data was used to calculate the data covariance. Two to three eigenvectors corresponding to the largest eigenvalues were used to calculate the signal subspace. The weight matrix was then calculated as a function of the forward lead field and the sensor data covariance and its signal subspace. The result is a full spatiotemporal reconstruction of estimated neural activity: a different spatial map exists for each latency, and likewise, for each spatial point (voxel) a full time-series can be extracted (often termed *virtual electrode*). The estimated neural location from any MEG inverse method is termed the *localization* of that source. We also determined the source orientation by computing the principle eigenvector of the source power output from the vector beamformer.

To put the monkey data into a standard normalized space we registered each animal's structural MRI to the 'AC-PC coordinate' frame using translations and rotations (no warping). This coordinate system is defined with the anterior commissure (AC) as the origin, the negative y-axis running through the posterior commissure (PC), and the positive z-axis running up through longitudinal cerebral fissure. For comparing the mediolateral variation across stimulation types and animals, the negative of the absolute value of the mediolateral coordinate was used since MK1 was stimulated on the left while the other three animals were stimulated on the right.

The source orientation was also converted from the individual structural MRI space to the 'AC-PC' coordinate frame so that orientations could be averaged across datasets/animals. The unit orientation vectors from all datasets of a stimulation type were averaged together. If they all pointed consistently in a particular direction, then the magnitude of this mean should equal 1, while completely randomly oriented vectors will sum to zero. However, in the case of limited sample size here (e.g. 4–12 vectors), the distribution varies with number of samples (vectors). Therefore we computed the distribution of means of groups of randomly-generated unit vectors (sample sizes 4, 5, 10 and 12) and determined the one-tailed 95% and 99.5% cut-offs for maximum values to test for significance.

The AC-PC coordinates of the voxel with largest MEG activation across space for the time peak of interest (~12 ms for digit, ~8 ms for lip, and ~50 ms for auditory stimulation) and the source power orientation were noted, as well as the actual peak latencies at that peak and other peaks if present. Significance of differences between the coordinates of the hand, face and auditory representations for both monkeys and humans were tested using two-tailed paired Student's t-tests corrected for family-wise errors (thus for three tests $p < 0.016$ was considered significant).

4.7. MEG processing — humans

Human MEG data were processed like the monkey CTF data (MK3 and MK4) using NUTMEG. The spherical homogeneous single-shell model was fitted to the scalp derived from the structural MRI. Individual trials with eye blinks or other artifacts were discarded prior to averaging and sources were estimated over a 2 mm-spaced 3D grid over a volume-of-interest (VOI). Due to computational limits, the VOI was smaller than a hemisphere (roughly one-tenth the whole brain volume), but large enough to encompass somatosensory and auditory cortex and surrounding regions. All sensors were used to reconstruct somatosensory activations, whereas only sensors on the hemisphere of interest were used for auditory data. Roughly 250 post-stimulus time points of non-filtered data were used to calculate the data covariance and two to three eigenvalues for the signal subspace.

The individual subject's structural MRI was normalized to MNI space using SPM2 (<http://www.fil.ion.ucl.ac.uk/spm>). The same spatial warping was then applied to the MEG reconstruction (as implemented in NUTMEG) and the MNI coordinate of the peak MEG voxel and source power orientation were noted as well as the peak latencies.

Acknowledgments

We thank Marianne Lowenthal, Susanne Honma, Anne Findlay, Evelyn Proctor, Kavita Vashi, Leighton Hinkley and Geoff Rau for assistance with data acquisition, Ron Bair-euther, Robert English-Fernandez, Patricia Ramsey and Grace Kim for assistance with anesthesia, and Sarang Dalal for comments on MEG processing. NIH funding was provided by R01 NS44590 to ED and SN, R01 DC4855 and R01 DC6435 to SN, and R01 NS35103 to LK.

REFERENCES

- Allison, T., McCarthy, G., Wood, C.C., Williamson, P.D., Spencer, D.D., 1989. Human cortical potentials evoked by stimulation of the median nerve. II. Cytoarchitectonic areas generating long-latency activity. *J. Neurophysiol.* 62, 711–722.
- Allison, T., McCarthy, G., Wood, C.C., Jones, S.J., 1991. Potentials evoked in human and monkey cerebral cortex by stimulation of the median nerve: a review of scalp and intracranial recordings. *Brain* 114, 2465–2503.
- Arezzo, J., Pickoff, A., Vaughan Jr., H.G., 1975. The sources and intracerebral distribution of auditory evoked potentials in the alert rhesus monkey. *Brain Res.* 90, 57–73.
- Arezzo, J.C., Vaughan, H.G., Legatt, A.D., 1981. Topography and intracranial sources of somatosensory evoked potentials in the monkey. II. Cortical components. *Electroencephalogr. Clin. Neurophysiol.* 51, 1–18.
- Barth, D.S., Sutherling, W., 1988. Current source-density and neuromagnetic analysis of the direct cortical response in rat cortex. *Brain Res.* 450, 280–294.
- Barth, D.S., Sutherling, W., Beatty, J., 1984. Fast and slow magnetic phenomena in focal epileptic seizures. *Science* 226, 855–857.

- Barth, D.S., Sutherling, W., Beatty, J., 1986. Intracellular currents of interictal penicillin spikes: evidence from neuromagnetic mapping. *Brain Res.* 368, 36–48.
- Bau Barth, D.S., Di, S., 1990. Three-dimensional analysis of auditory-evoked potentials in rat neocortex. *J. Neurophysiol.* 64, 1527–1536.
- Baumgartner, C., Barth, D.S., Levesque, M.F., Sutherling, W.W., 1992. Human hand and lip sensorimotor cortex as studied on electrocorticography. *Electroencephalogr. Clin. Neurophysiol.* 84, 115–126.
- Brugge, J.F., Merzenich, M.M., 1973. Responses of neurons in auditory cortex of the macaque monkey to monaural and binaural stimulation. *J. Neurophysiol.* 36, 1138–1158.
- Buchner, H., Fuchs, M., Wischmann, H.A., Dossel, O., Ludwig, I., Knepper, A., Berg, P., 1994. Source analysis of median nerve and finger stimulated somatosensory evoked potentials: multichannel simultaneous recording of electric and magnetic fields combined with 3D-MR tomography. *Brain Topogr.* 6, 299–310.
- Caminiti, R., Ghaziri, H., Galuske, R., Hof, P.R., Innocenti, G.M., 2009. Evolution amplified processing with temporally dispersed slow neuronal connectivity in primates. *PNAS* 106, 19551–19556.
- Casper, S., Geyer, S., Schleicher, A., Mohlberg, A., Amunts, K., Zilles, K., 2006. The human inferior parietal cortex: cytoarchitectonic parcellation and interindividual variability. *NeuroImage* 33, 430–448.
- Celesia, G.G., 1976. Organization of auditory cortical areas in man. *Brain* 99, 403–414.
- Chait, M., Simon, J.Z., Poeppel, D., 2004. Auditory M50 and M100 responses to broadband noise: functional implications. *NeuroReport* 15, 2455–2458.
- Cuffin, B.N., Cohen, D., 1979. Comparison of the magnetoencephalogram and electroencephalogram. *Electroencephalogr. Clin. Neurophysiol.* 47, 132–146.
- Dalal, S.S., Zumer, J.M., Agrawal, V., Hild, K.E., Sekihara, K., Nagarajan, S.S., 2004. NUTMEG: a neuromagnetic source reconstruction toolbox. *Neurol. Clin. Neurophysiol.* 2004, 52.
- Dalal, S.S., Guggisberg, A.G., Edwards, E., Sekihara, K., Findlay, A.M., Canolty, R.T., Berger, M.S., Knight, R.T., Barbaro, N.M., Kirsch, H.E., Nagarajan, S.S., 2008. Five-dimensional neuroimaging: localization of the time–frequency dynamics of cortical activity. *NeuroImage* 40, 1686–1700.
- Disbrow, E., Roberts, T., Poeppel, D., Krubitzer, L., 2001. Evidence for interhemispheric processing of inputs from the hands in human S2 and PV. *J. Neurophysiol.* 85, 2236–2244.
- Disbrow, E.A., Hinkley, L.B., Roberts, T.P., 2003. Ipsilateral representation of oral structures in human anterior parietal somatosensory cortex and integration of inputs across the midline. *J. Comp. Neurol.* 467, 487–495.
- Edgar, J.C., Huang, M.X., Weisend, M.P., Sherwood, A., Miller, G.A., Adler, L.E., Canive, J.M., 2003. Interpreting abnormality: an EEG and MEG study of P50 and the auditory paired-stimulus paradigm. *Biol. Psych.* 65, 1–20.
- Eyre, J.A., Miller, S., Ramesh, V., 1991. Constancy of central conduction delays during development in man: investigation of motor and somatosensory pathways. *J. Physiol.* 434, 441–452.
- Forss, N., Salmelin, R., Hari, R., 1994. Comparison of somatosensory evoked fields to airpuff and electric stimuli. *Electroencephalogr. Clin. Neurophysiol.* 92, 510–517.
- Fuchs, M., Wagner, M., Wischmann, H.A., Kohler, T., Theissen, A., Drenkhahn, R., Buchner, H., 1998. Improving source reconstructions by combining bioelectric and biomagnetic data. *Electroencephalogr. Clin. Neurophysiol.* 107, 93–111.
- Gaetz, W.C., Cheyne, D.O., 2003. Localization of human somatosensory cortex using spatially filtered magnetoencephalography. *Neurosci. Lett.* 340, 161–164.
- Gardner, E.P., Hämäläinen, H.A., Warren, S., Davis, J., Young, W., 1984. Somatosensory evoked potentials (SEPs) and cortical single unit responses elicited by mechanical tactile stimuli in awake monkeys. *Electroencephalogr. Clin. Neurophysiol.* 58, 537–552.
- Godey, B., Schwartz, D., de Graaf, J.B., Chauvel, P., Liegeois-Chauvel, C., 2001. Neuromagnetic source localization of auditory evoked fields and intracerebral evoked potentials: a comparison of data in the same patients. *Clin. Neurophysiol.* 112, 1850–1859.
- Gutierrez, D., Nehorai, A., Dogandzic, A., 2006. Performance analysis of reduced-rank beamformers for estimating dipole source signals using EEG/MEG. *IEEE Trans. Biomed. Eng.* 53, 840–844.
- Hackett, T.A., 2007. Organization and correspondence of the auditory cortex of humans and nonhuman primates. In: Kaas, J., Preuss, T. (Eds.), *The Evolution of Nervous Systems*. Academic Press, Oxford, pp. 109–119.
- Hackett, T.A., Preuss, T.M., Kaas, J.H., 2001. Architectonic identification of the core region in auditory cortex of macaques, chimpanzees, and humans. *J. Comp. Neurol.* 441, 197–222.
- Halgren, E., 2004. How can intracranial recordings assist MEG source localization? *Neurol. Clin. Neurophysiol.* 2004, 86.
- Hamada, Y., Watanabe, T., Chatani, K., Hayakawa, S., Iwamoto, M., 2005. Morphometrical comparison between Indian- and Chinese-derived rhesus macaques (*Macaca mulatta*). *Anthrop. Sci.* 113, 183–188.
- Hämäläinen, H., Kekoni, J., Sams, M., Reinikainen, K., Naatanen, R., 1990. Human somatosensory evoked potentials to mechanical pulses and vibration: contributions of SI and SII somatosensory cortices to P50 and P100 components. *Electroencephalogr. Clin. Neurophysiol.* 75, 13–21.
- Hämäläinen, M., Hari, R., Ilmoniemi, R.J., Knuutila, J., Lounasmaa, O.V., 1993. Magnetoencephalography — theory, instrumentation, and applications to noninvasive studies of the working human brain. *Rev. Modern Phys.* 65, 413.
- Hari, R., Hämäläinen, M., Kaukoranta, E., Reinikainen, K., Teszner, D., 1983. Neuromagnetic responses from the second somatosensory cortex in man. *Acta Neurol. Scand.* 68, 207–212.
- Hari, R., Reinikainen, K., Kaukoranta, E., Hämäläinen, M., Ilmoniemi, R., Penttinen, A., Salminen, J., Teszner, D., 1984. Somatosensory evoked cerebral magnetic fields from SI and SII in man. *Electroencephalogr. Clin. Neurophysiol.* 57, 254–263.
- Hashimoto, I., Mashiko, T., Kimura, T., Imada, T., 1999. Are there discrete distal–proximal representations of the index finger and palm in the human somatosensory cortex? A neuromagnetic study. *Clin. Neurophysiol.* 110, 430–437.
- Hoshiyama, M., Kakigi, R., Koyama, S., Kitamura, Y., Shimojo, M., Watanabe, S., 1996. Somatosensory evoked magnetic fields following stimulation of the lip in humans. *Electroencephalogr. Clin. Neurophysiol.* 100, 96–104.
- Jacobson, G.P., Ahmad, B.K., Moran, J., Newman, C.W., Tepley, N., Wharton, J., 1991. Auditory evoked cortical magnetic field (M100–M200) measurements in tinnitus and normal groups. *Hear. Res.* 56, 44–52.
- Kaas, J.H., 1983. What, if anything, is SI? Organization of first somatosensory area of cortex. *Physiol. Rev.* 63, 206–231.
- Kaas, J.H., 1993. The functional organization of somatosensory cortex in primates. *Ann. Anat.* 175, 509–518.
- Kaas, J.H., Nelson, R.J., Sur, M., Lin, C.S., Merzenich, M.M., 1979. Multiple representations of the body within the primary somatosensory cortex of primates. *Science* 204, 521–523.
- Kekoni, J., Tiihonen, J., Hämäläinen, H., 1992. Fast decrement with stimulus repetition in ERPs generated by neuronal systems involving somatosensory SI and SII cortices: electric and magnetic evoked response recordings in humans. *Int. J. Psychophysiol.* 12, 281–288.
- Krubitzer, L.A., Disbrow, E.A., 2008. The evolution of parietal areas involved in hand use in primates. In: Gardner, E., Kaas, J. (Eds.), *Somatosensation*. Elsevier, London, pp. 183–214.
- Krubitzer, L.A., Huffman, K.J., Disbrow, E.A., Recanzone, G., 2004. Organization of area 3a in macaque monkeys: contributions to the cortical phenotype. *J. Comp. Neurol.* 471, 97–111.

- Kulics, A.T., Cauller, L.J., 1986. Cerebral cortical somatosensory evoked responses, multiple unit activity and current source-densities: their interrelationships and significance to somatic sensation as revealed by stimulation of the awake monkey's hand. *Exp. Brain Res.* 62, 46–60.
- Kyuhou, S., Okada, Y.C., 1993. Detection of magnetic evoked fields associated with synchronous population activities in the transverse CA1 slice of the guinea pig. *J. Neurophysiol.* 70, 2665–2668.
- Leahy, R.M., Mosher, J.C., Spencer, M.E., Huang, M.X., Lewine, J.D., 1998. A study of dipole localization accuracy for MEG and EEG using a human skull phantom. *Electroencephalogr. Clin. Neurophysiol.* 107, 159–173.
- Liegeois-Chauvel, C., Musolino, A., Badier, J.M., Marquis, P., Chauvel, P., 1994. Evoked potentials recorded from the auditory cortex in man: evaluation and topography of the middle latency components. *Electroencephalogr. Clin. Neurophysiol.* 92, 204–214.
- Lopez, L., Chan, C.Y., Okada, Y.C., Nicholson, C., 1991. Multimodal characterization of population responses evoked by applied electric field in vitro: extracellular potential, magnetic evoked field, transmembrane potential, and current-source density analysis. *J. Neurosci.* 11, 1998–2010.
- McCarthy, G., Allison, T., 1995. Trigeminal evoked potentials in somatosensory cortex of the *Macaca mulatta*. *J. Neurosurg.* 82, 1015–1020.
- McCarthy, G., Wood, C.C., Allison, T., 1991. Cortical somatosensory evoked potentials. I. Recordings in the monkey *Macaca fascicularis*. *J. Neurophysiol.* 66, 53–63.
- Morel, A., Garraghty, P.E., Kaas, J.H., 1993. Tonotopic organization, architectonic fields, and connections of auditory cortex in macaque monkeys. *J. Comp. Neurol.* 335, 437–459.
- Nagamine, T., Makela, J., Mima, T., Mikuni, N., Nishitani, N., Satoh, T., Ikeda, A., Shibasaki, H., 1998. Serial processing of the somesthetic information revealed by different effects of stimulus rate on the somatosensory-evoked potentials and magnetic fields. *Brain Res.* 791, 200–208.
- Nakahara, H., Nakasato, N., Kanno, A., Murayama, S., Hatanaka, K., Itoh, H., Yoshimoto, T., 2004. Somatosensory-evoked fields for gingiva, lip, and tongue. *J. Dent. Res.* 83, 307–311.
- Nakamura, A., Yamada, T., Goto, A., Kato, T., Ito, K., Abe, Y., Kachi, T., Kakigi, R., 1998. Somatosensory homunculus as drawn by MEG. *NeuroImage* 7, 377–386.
- Nelson, R.J., Sur, M., Felleman, D.J., Kaas, J.H., 1980. Representations of the body surface in postcentral parietal cortex of *Macaca fascicularis*. *J. Comp. Neurol.* 192, 611–643.
- Okada, Y.C., Nicholson, C., 1988. Magnetic evoked field associated with transcortical currents in turtle cerebellum. *Biophys. J.* 53, 723–731.
- Okada, Y., Lauritzen, M., Nicholson, C., 1987a. MEG source models and physiology. *Phys. Med. Biol.* 32, 43–51.
- Okada, Y.C., Lauritzen, M., Nicholson, C., 1987b. Magnetic field associated with neural activities in an isolated cerebellum. *Brain Res.* 412, 151–155.
- Okada, Y.C., Lauritzen, M., Nicholson, C., 1988. Magnetic field associated with spreading depression: a model for the detection of migraine. *Brain Res.* 442, 185–190.
- Okada, Y.C., Wu, J., Kyuhou, S., 1997. Genesis of MEG signals in a mammalian CNS structure. *Electroencephalogr. Clin. Neurophysiol.* 103, 474–485.
- Pantev, C., Hoke, M., Lehnertz, K., Lutkenhoner, B., Fahrendorf, G., Stoher, U., 1990. Identification of sources of brain neuronal activity with high spatiotemporal resolution through combination of neuromagnetic source localization (NMSL) and magnetic resonance imaging (MRI). *Electroencephalogr. Clin. Neurophysiol.* 75, 173–184.
- Patterson, R.D., Uppenkamp, S., Johnsrude, I.S., Griffiths, T.D., 2002. The processing of temporal pitch and melody information in auditory cortex. *Neuron* 36, 767–776.
- Penfield, W., Boldrey, E., 1937. Somatic motor and sensory representation in the cerebral cortex of man as studied by electrical stimulation. *Brain* 60, 389–443.
- Powell, T.P., Mountcastle, V.B., 1959. Some aspects of the functional organization of the cortex of the postcentral gyrus of the monkey: a correlation of findings obtained in a single unit analysis with cytoarchitecture. *Bull. Johns Hopkins Hosp.* 105, 133–162.
- Rauschecker, J.P., Tian, B., 2004. Processing of band-passed noise in the lateral auditory belt cortex of the rhesus monkey. *J. Neurophysiol.* 91, 2578–2589.
- Rauschecker, J.P., Tian, B., Hauser, M., 1995. Processing of complex sounds in the macaque nonprimary auditory cortex. *Science* 268, 111–114.
- Reite, M., Teale, P., Zimmerman, J., Davis, K., Whalen, J., 1988. Source location of a 50 msec latency auditory evoked field component. *Electroencephalogr. Clin. Neurophysiol.* 70, 490–498.
- Roland, P.E., Zilles, K., 1998. Structural divisions and functional fields in the human cerebral cortex. *Brain Res. Brain Res. Rev.* 26, 87–105.
- Sekihara, K., Nagarajan, S.S., Poeppel, D., Marantz, A., Miyashita, Y., 2001. Reconstructing spatio-temporal activities of neural sources using an MEG vector beamformer technique. *IEEE Trans. Biomed. Eng.* 48, 760–771.
- Sekihara, K., Nagarajan, S.S., Poeppel, D., Marantz, A., 2002. Performance of an MEG adaptive-beamformer technique in the presence of correlated neural activities: effects on signal intensities and time course estimates. *IEEE Trans. Biomed. Eng.* 49, 1534–1546.
- Sharon, D., Hämäläinen, M.S., Tootell, R.B.H., Halgren, E., Belliveau, J.W., 2007. The advantage of combining MEG and EEG: comparison to fMRI in focally stimulated visual cortex. *NeuroImage* 36, 1225–1235.
- Sutherling, W.W., Crandall, P.H., Darcey, T.M., Becker, D.P., Levesque, M.F., Barth, D.S., 1988. The magnetic and electric fields agree with intracranial localizations of somatosensory cortex. *Neurology* 38, 1705–1714.
- Teale, P., Delmore, J., Simon, J., Reite, M., 1994. Magnetic auditory imaging in macaque monkey. *Brain Res. Bull.* 33, 615–620.
- Wessinger, C.M., VanMeter, J., Tian, B., Van Lare, J., Pekar, J., Rauschecker, J.P., 2001. Hierarchical organization of the human auditory cortex revealed by functional magnetic resonance imaging. *J. Cogn. Neurosci.* 13, 1–7.
- Wilson, T.W., Godwin, D.W., Ctozy, P.W., Nader, M.A., Kraft, R.A., Buchheimer, N.C., Daunais, J.B., 2009. A MEG investigation of somatosensory processing in rhesus monkey. *NeuroImage* 46, 998–1003.
- Wood, C.C., Spencer, D.D., Allison, T., McCarthy, G., Williamson, P.D., Goff, W.R., 1988. Localization of human sensorimotor cortex during surgery by cortical surface recording of somatosensory evoked potentials. *J. Neurosurg.* 68, 99–111.
- Wu, J., Okada, Y.C., 1998. Physiological bases of the synchronized population spikes and slow wave of the magnetic field generated by a guinea-pig longitudinal CA3 slice preparation. *Electroencephalogr. Clin. Neurophysiol.* 107, 361–373.
- Zhu, Z., Zumer, J.M., Lowenthal, M.E., Padberg, J., Recanzone, G.H., Krubitzer, L.A., Nagarajan, S.N., Disbrow, E.A., 2009. The relationship between magnetic and electrophysiological responses to complex tactile stimuli. *BMC Neurosci.* 10, 4.